

---

# Rao-Blackwellising Bayesian Causal Inference

---

Christian Toth<sup>1</sup>

Christian Knoll<sup>1,2</sup>

Franz Pernkopf<sup>1</sup>

Robert Peharz<sup>1</sup>

<sup>1</sup>Graz University of Technology

<sup>2</sup>Levata GmbH

## Abstract

Bayesian causal inference, i.e., inferring a posterior over causal models for the use in downstream causal reasoning tasks, poses a hard computational inference problem that is little explored in literature. In this work, we combine techniques from order-based MCMC structure learning with recent advances in gradient-based graph learning into an effective Bayesian causal inference framework. Specifically, we decompose the problem of inferring the causal structure into (i) inferring a topological order over variables and (ii) inferring the parent sets for each variable. When limiting the number of parents per variable, we can exactly marginalise over the parent sets in polynomial time. We further use Gaussian processes to model the unknown causal mechanisms, which also allows their exact marginalisation. This introduces a Rao-Blackwellization scheme, where all components are eliminated from the model, except for the causal order, for which we learn a distribution via gradient-based optimisation. The combination of Rao-Blackwellization with our sequential inference procedure for causal orders yields state-of-the-art on linear and non-linear additive noise benchmarks with scale-free and Erdos-Renyi graph structures.

## 1 INTRODUCTION

In recent work, [Toth et al. \[2022\]](#) pointed out, that the classical separation of causal discovery and causal reasoning into distinct, consecutive tasks does not account for the epistemic uncertainty about the causal structure during the causal reasoning phase. Moreover, [Gradu et al. \[2022\]](#) show that reusing data during the reasoning phase that has already been used for the causal discovery task may yield

biased results. To address these issues, [Toth et al. \[2022\]](#) propose to infer a Bayesian posterior over some causal quantity of interest, such as an average treatment effect, the presence of a causal connection, or the full causal graph, by marginalising over posterior structural causal models (SCMs).

Although this is a conceptually appealing approach subsuming both Bayesian causal discovery and reasoning, posterior inference over entire SCMs is in general intractable. Hence, most research focuses on the on the (still hard) sub-problem of causal structure learning. While classical MCMC-based approaches to structure learning often decompose DAG learning into (i) learning a topological variable order and (ii) conditional on the order, learning the parent sets for each variable [[Koller and Friedman, 2003](#), [Koivisto and Sood, 2004](#)], recent gradient-based DAG structure learning techniques focuses on soft acyclicity constraints or uses topological orders only as a vehicle to sample DAGs. Surprisingly, a combination of these two approaches has been little explored in the literature.

In this work, we close this gap by combining the best of both worlds: we employ gradient-based optimisation to learn a distribution over causal orders, and, by limiting the number of parents per variable, we can perform exact inference over parent sets in polynomial time. We further use Gaussian processes to model the unknown causal mechanisms, which also allows their exact marginalisation. This effectively introduces a Rao-Blackwellization scheme, where all components are eliminated from the model, except for the causal order. Combining this with a sequential inference procedure over topological order yields state-of-the-art estimation results on linear and non-linear additive noise benchmarks with scale-free and Erdos-Renyi graph structures. Our main contributions are:

- We propose an effective Bayesian causal inference framework by Rao-Blackwellising the hard problem of Bayesian causal inference and show its practical superiority in simulated benchmarks.

- Interpreting our estimation procedure from the perspective of importance sampling, we analyse the requirements of the involved proposal distribution over parent sets and causal orders. We argue that these considerations are likewise relevant to variational inference-based approaches.
- We provide a modular Python-based implementation of our inference framework to the community.

## 2 BACKGROUND

### 2.1 STRUCTURAL CAUSAL MODELS

The mathematical treatment of causal questions requires a well-posed model. One of the most prominent causal models is the structural causal model (SCM) [Pearl, 2009]:

**Definition 2.1** (SCM). An SCM  $\mathcal{M}$  over observed endogenous variables  $\mathbf{X} = \{X_1, \dots, X_d\}$  and unobserved exogenous variables  $\mathbf{U} = \{U_1, \dots, U_d\}$  consists of structural equations, or mechanisms,

$$X_i := f_i(\mathbf{Pa}_i, U_i), \quad \text{for } i \in \{1, \dots, d\}, \quad (2.1)$$

which assign the value of each  $X_i$  as a deterministic function  $f_i$  of its direct causes, or causal parents,  $\mathbf{Pa}_i \subseteq \mathbf{X} \setminus \{X_i\}$  and an exogenous variable  $U_i$ , and a joint distribution  $p(\mathbf{U})$  over the exogenous variables.

Associated with each SCM is a directed acyclic graph (DAG)  $G$  induced by the set of parent sets  $\mathbf{Pa} = \{\mathbf{Pa}_i\}_{i=1}^d$  with vertices  $\mathbf{X}$  and edges  $X_j \rightarrow X_i$  if and only if  $X_j \in \mathbf{Pa}_i$ . Any acyclic SCM then induces a unique observational distribution  $p(\mathbf{X} | \mathcal{M})$  over the endogenous variables  $\mathbf{X}$ , which is obtained as the pushforward measure of  $p(\mathbf{U})$  through the causal mechanisms in Eq. (2.1).

### 2.2 CAUSAL ORDERS

A permutation  $L = \langle L_1, \dots, L_d \rangle$  of the endogenous variables  $\mathbf{X} = \bigcup_{i=1}^d \{L_i\}$ , where  $L_i \neq L_j$  for all  $i \neq j$ , entails a strict total order among  $L_1 \prec L_2 \prec \dots \prec L_d$  the variables. Henceforth, we refer to such a permutation  $L$  as a *causal order*. A causal order  $L$  constrains the possible causal interactions between the causal variables, i.e.,  $X_i$  can be a (direct) cause of  $X_j$  if, and only if,  $X_i \prec X_j$  in  $L$ .

We define  $L_{<k} = \langle L_1, \dots, L_{k-1} \rangle$  to be the first  $k-1$  elements in  $L$  and let  $[L_{<k}] = \bigcup_{i=1}^{k-1} \{L_i\}$ . We will often use vectors of length  $d$ , for example  $\theta = (\theta_1, \dots, \theta_d)$ , whose entries correspond to endogenous variables. We will index such vectors by a subset of  $\mathbf{X}$  to form a sub-vector, for example  $\theta_{[L_{<k}]} = (\theta_i | X_i \in [L_{<k}])$ .

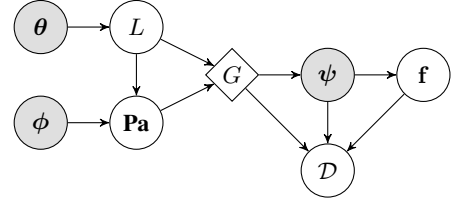


Figure 1: Bayesian network view of our proposed inference framework. We infer the posterior parameters  $\theta$  and  $\phi$  of a parameterised joint distribution  $p(L, \mathbf{Pa} | \theta, \phi)$  over causal orders  $L$  and (unconstrained) parent sets  $\mathbf{Pa}$ . Our model factorises the joint into the marginal over causal orders  $p(L | \theta)$ , and the conditional over unconstrained parent sets  $p(\mathbf{Pa} | L, \phi)$ . The causal DAG  $G = M^L \odot \mathbf{Pa}$  is deterministically computed by element-wise multiplication of the adjacency mask induced by  $L$ , and the unconstrained parent set matrix  $\mathbf{Pa}$ . For a fixed maximum cardinality of the parent sets, we marginalise over DAGs by exhaustively enumerating all possible parent sets (which obsoletes inference of  $\phi$ ). Additionally, we infer the posterior parameters  $\psi$  of the parameterised joint distribution over mechanisms and noise variables  $p(\mathbf{f}, \mathbf{U} | \psi)$ . In our case,  $\psi$  are the hyperparameters of a set of Gaussian Processes, but they could also be the parameters of a neural network, etc. Mechanisms, noise distribution and graph together give rise to the data-generating likelihood  $p(\mathcal{D} | \mathbf{f}, \psi, G)$ .

Let  $\lambda^L: \mathbf{X} \mapsto \{1, \dots, d\}$  be the bijective mapping between  $\mathbf{X}$  and indices in  $L$ , i.e.,  $\lambda^L(X_i) = k \iff L_k = X_i$ . We denote by  $Q^L \in \{0, 1\}^{d \times d}$  the *permutation matrix* representing  $L$ , where  $Q_{ij}^L = 1$  iff  $\lambda^L(X_i) = j$ . Further, we denote by  $M^L \in \{0, 1\}^{d \times d}$  the *adjacency mask* induced by  $L$ , where  $M_{ij}^L = 1$  iff  $\lambda^L(X_i) < \lambda^L(X_j)$ .

## 3 BAYESIAN CAUSAL INFERENCE VIA CAUSAL ORDERS

The Bayesian causal inference problem [Toth et al., 2022] is to infer a Bayesian query posterior

$$p(Y | \mathcal{D}) = \mathbb{E}_{\mathcal{M} | \mathcal{D}} [p(Y | \mathcal{M})] \quad (3.1)$$

by marginalising over posterior SCMs given a set of (observational)<sup>1</sup> data  $\mathcal{D} = \{\mathbf{x}_n \stackrel{\text{i.i.d.}}{\sim} p(\mathbf{X} | \mathcal{M}^*)\}_{n=1}^N$  collected from the true underlying SCM  $\mathcal{M}^*$ . The query  $Y$  could be, e.g., an average treatment effect or the full causal graph. In general, the marginalisation over SCMs is intractable and poses the key computational challenge for Bayesian causal inference. For our inference framework as described in

<sup>1</sup>While our framework and implementation can handle interventional data, we do not evaluate this scenario experimentally because not all baselines support the use of interventional data, and the observational case is the more difficult problem from the perspective of model identifiability.

Fig. 1, an SCM is parameterised as a triple  $\mathcal{M} = (G, \mathbf{f}, \psi)$  of the causal graph  $G$ , the causal mechanisms  $\mathbf{f}$ , and the parameters of mechanisms and exogenous noise distributions  $\psi$ . Thus, an expectation w.r.t. SCMs as in Eq. (3.1) can be written as an importance weighted expectation (see Appx. A)

$$\mathbb{E}_{\mathcal{M} | \mathcal{D}} [Y(\mathcal{M})] = \mathbb{E}_{\theta, \phi, \psi | \mathcal{D}} \left[ \mathbb{E}_{L | \theta} \left[ \mathbb{E}_{G | L, \phi} \left[ w \cdot \mathbb{E}_{\mathbf{f} | \psi, \mathcal{D}} [Y(\mathcal{M})] \right] \right] \right] \quad (3.2)$$

where

$$w := \frac{p(\mathcal{D} | \psi, G) \cdot p(\psi | G)}{\mathbb{E}_{L' | \theta} \left[ \mathbb{E}_{G' | L', \phi} [p(\mathcal{D} | \psi, G') \cdot p(\psi | G')] \right]}. \quad (3.3)$$

This formulation, inspired by Lorch et al. [2021], transforms inference over SCMs into the problem of inferring posterior parameters  $p(\theta, \phi, \psi | \mathcal{D})$  of a generative model, as laid out in Fig. 1. The so-learned parameterised distribution over causal graphs  $p(G | \theta, \phi) = \mathbb{E}_{L | \theta} [p(G | L, \phi)]$  appearing in Eq. (3.2) can be interpreted as a proposal distribution,<sup>2</sup> and the  $w$  as defined in Eq. (3.3) as importance weight. Thus, to practically estimate the expectation in Eq. (3.2), we use a simple Monte-Carlo estimator, by drawing proposal SCMs from our generative model and weighting their query value  $Y(\mathcal{M})$  according to their importance weights.

Ensuring that our proposal distributions are sufficiently expressive, it suffices to infer a maximum a posteriori (MAP) estimate of the posterior parameters  $\theta, \phi, \psi$  via gradient-based optimisation by maximising the log-posterior:

$$\nabla \log p(\theta, \phi, \psi | \mathcal{D}) = \nabla \log p(\theta, \phi) + \nabla \log \mathbb{E}_{\mathbf{Pa}, L | \theta, \phi} [p(\mathcal{D}, \psi | G)]. \quad (3.4)$$

A major issue for the training of such a model is the quality of the gradient estimation in the face of the high-dimensional problem space. Likewise, using a Monte-Carlo estimate of Eq. (3.2) may suffer from high variance. To mitigate these issues, we now propose several ways to Rao-Blackwellise our inference procedure.

### 3.1 RAO-BLACKWELLIZING THE INFERENCE PROCEDURE

We defer derivations and proofs in the context of this section to Appx. A.

#### 3.1.1 Mechanism Inference

To compute the importance weights in Eq. (3.3) we have to compute the marginal log-likelihood

$$p(\mathcal{D} | \psi, G) = \mathbb{E}_{\mathbf{f} | \psi, G} [p(\mathcal{D} | \mathbf{f}, \psi, G) \cdot p(\mathbf{f} | \psi)], \quad (3.5)$$

<sup>2</sup>Note, that the learned distributions are **not** per-se the actual posterior distribution, although they would be optimal proposals if they were.

which is intractable in general. As we focus on (non-)linear additive noise models in this work, we follow [Toth et al., 2022] and model each mechanisms via a distinct Gaussian process (GP), assuming homoscedastic Gaussian noise and causal sufficiency. The advantage of using GPs is, that the in general intractable likelihood

$$p(\mathcal{D}_i | \psi_i, G) = \mathbb{E}_{\mathbf{f} | \psi_i, G} [p(\mathcal{D}_i | \mathbf{f}_i, \psi_i, G)] \quad (3.6)$$

can be computed in closed form. The same holds true for the predictive posterior  $p(\mathcal{D}_i^{\text{test}} | \psi_i, G, \mathcal{D})$  possibly needed in Eq. (3.2).

We factorise the GP hyper-parameter prior<sup>3</sup> and the likelihood over parent sets for each node  $i$ , i.e.,

$$p(\mathcal{D} | \psi, G) \cdot p(\psi | G) = \prod_i p(\mathcal{D}_i | \psi_i, G) \cdot p(\psi_i | \mathbf{Pa}_i^G), \quad (3.7)$$

allowing for efficient computation by caching intermediate results. To infer the individual GP hyper-parameters we perform for a MAP-Type II estimation by performing gradient-ascent on

$$\nabla_{\psi_i} \log p(\psi_i | \mathcal{D}, G) = \nabla_{\psi_i} p(\mathcal{D}_i | \psi_i, G) + \nabla_{\psi_i} p(\psi_i | G). \quad (3.8)$$

For root nodes, i.e., nodes without parents, we place a conjugate normal-inverse-gamma prior on the mean and variance of that node, which also allows for closed-form inference.

#### 3.1.2 Parent Set Inference

The marginalisation w.r.t. parent sets in Eqs. (3.2) and (3.4) poses a hard combinatorial problem. Although, the number of DAGs consistent with any given (causal) order is  $2^{\frac{d \cdot (d-1)}{2}}$  and as such significantly smaller than the total number of DAGs with  $d$  nodes, which grows super-exponentially in  $d$  (see [OEIS Foundation Inc., 2024]). Thus, an exhaustive enumeration of DAGs is still infeasible.

In this work, we explore two different ways of tackling this problem. First, by restricting the number of parents per variable, i.e. introducing a cardinality constraints on the parent sets, we can tractably compute the expectation w.r.t. parent sets via exhaustive enumeration. Second, we propose a tractable and expressive proposal distribution  $p(\mathbf{Pa} | L, \phi)$  over *unrestricted* parent sets  $\mathbf{Pa}$  conditional on a causal order  $L$  that we use to compute Monte Carlo estimates.

<sup>3</sup>The parameter set  $\psi_i$  contains the GP's kernel parameters and the noise variance. Note that, other than the structural dependence on the parent sets, the prior parameters  $\psi$  are independent of  $\phi$  and  $\theta$ .

**Exhaustive Enumeration of Parent Sets.** By restricting the maximum size of any admissible parent set to some integer  $K$ , the number of distinct parent sets consistent with any causal order  $L$  is polynomial in  $K$ . Although the exhaustive enumeration of all DAGs with restricted parent set size is still infeasible, it turns out, that given a causal order, the expectation w.r.t. graphs can be tractably computed for quantities  $Y(G)$  that decompose over the parent sets.

**Proposition 3.1.** *Let  $Y(G) = \prod_i Y_i(\mathbf{Pa}_i^G)$  and  $w(G) = \prod_i w(\mathbf{Pa}_i^G)$  be factorising over the parent sets, then we can compute*

$$\mathbb{E}_{G|L} [w(G)Y(G)] = \prod_i \sum_{\mathbf{Pa}_i} p(\mathbf{pa}_i | L) w_i(\mathbf{pa}_i) Y_i(\mathbf{Pa}_i). \quad (3.9)$$

Additionally,

**Proposition 3.2.** *Let  $Y(G) = \sum_i Y_i(\mathbf{Pa}_i^G)$  be summing and  $w(G) = \prod_i w(\mathbf{Pa}_i^G)$  be factorising over the parent sets, then we can compute*

$$\mathbb{E}_{G|L} [w(G)Y(G)] = \sum_i \left( \prod_{j \neq i} \alpha_j(L) \right) \cdot \sum_{\mathbf{Pa}_i} p(\mathbf{pa}_i | L) w_i(\mathbf{pa}_i) Y_i(\mathbf{Pa}_i), \quad (3.10)$$

where

$$\alpha_j(L) = \sum_{\mathbf{Pa}_i} p(\mathbf{pa}_i, L) w_i(\mathbf{pa}_i).$$

These propositions generalises the results presented by [Koller and Friedman \[2003\]](#), [Koivisto and Sood \[2004\]](#) on how to compute the posterior probabilities of edges or parent sets, which is a special case of Prop. 3.1, to our setting of Bayesian causal inference where  $w$  will be the importance weights as in Eq. (3.3). In practice, we assume a uniform prior  $p(\mathbf{Pa}_i | L)$  over parent sets consistent with a given causal order.

**An Expressive Distribution over Parent Sets.** As the restriction of the maximum parent set sizes may violate the reality of the true underlying causal graph to be inferred, we propose to learn a tractable and expressive proposal distribution  $p(\mathbf{Pa} | L, \phi)$  over parent sets which is amenable to gradient-based optimisation. Importantly,  $p(\mathbf{Pa} | L, \phi)$  models a distribution over parent sets that are unrestricted in cardinality, and possibly form a cyclic graph. Combining the causal order  $L$  with such parent sets, we can deterministically compute the adjacency matrix of an acyclic graph  $G = M^L \cdot \mathbf{Pa}$  by element-wise multiplication of the adjacency mask  $M^L$  induced by the causal order, and the adjacency matrix  $\mathbf{Pa}$  induced by the parent sets. Using the

---

### Algorithm 1: Sample Parent Sets

---

**Input:** Logit function

$$h_\phi : \mathbb{R}^{d \times d} \mapsto (\mathbb{R}^M, \mathbb{R}^{M \times d \times K}, \mathbb{R}^{d \times K \times d})$$

**Output:** Parent sets  $\mathbf{Pa}$  sampled from  $p(\mathbf{Pa} | L, \phi)$

$\phi_{\text{TLM}}, \phi_{\text{MOM}}, \phi_{\text{MN}} \leftarrow h(Q^L)$  ▷Step I

$m \sim \text{CAT}(\phi_{\text{TLM}})$  ▷Step II

$k \sim \text{CAT}(\phi_{\text{MOM}}[m])$  ▷Step III

$\mathbf{Pa} \leftarrow \{\mathbf{pa}_i \sim \text{MN}(\mathbf{Pa}_i | \phi_{\text{MN}}[i, k])\}$  ▷Step IV

---

score-function estimator, the gradient in Eq. (3.4) w.r.t.  $\phi$  can be estimated as

$$\nabla_\phi \log p(\theta, \phi, \psi | \mathcal{D}) = \nabla_\phi \log p(\phi) + \mathbb{E}_{L|\theta} [\mathbb{E}_{\mathbf{Pa}|L,\phi} [w \cdot \nabla_\phi p(\mathbf{Pa} | L, \phi)]] . \quad (3.11)$$

with  $w$  as defined in Eq. (3.3).

When designing any proposal distribution, note that the optimal choice would be the actual target distribution. In our case, this would coincide with the true posterior over DAGs. Hence, we should ask ourselves the question, what kind of structural properties the true DAG posterior may exhibit, in order to design a proposal distribution that can, at least in principle, *reasonably* approximate it. Clearly, the same considerations apply to the design of a variational distribution used in the context of variational inference.

We argue, that the convenient and commonly made choice [[Zheng et al., 2018](#), [Brouillard et al., 2020](#), [Cundy et al., 2021](#), [Charpentier et al., 2022](#)] of modeling the graph posterior as a set of independent Bernoulli edge distributions may fail even in simple cases. Consider the canonical example where the causal chain graph  $G_1 : X \rightarrow Y \rightarrow Z$  is not identifiable from observational data. The fork  $G_2 : X \leftarrow Y \rightarrow Z$  and the reverse chain  $G_3 : X \leftarrow Y \leftarrow Z$  are in the same Markov equivalence class (MEC). In the limit of infinite data, the graph posterior will collapse onto the MEC, all elements having the same posterior probability. However, for the independent Bernoulli parametrisation, it is impossible to represent the true DAG posterior. By assigning each edge present in the MEC a positive probability, we identify two pathologies. First, the model fails to represent a distribution over disjoint parent sets, e.g., the true parent sets of  $Y$  may be  $\{X\}$  or  $\{Z\}$ , but *not*  $\{X, Z\}$ . Second, the parent sets of the individual nodes are coupled in so far, as they must jointly entail an acyclic graph, which is clearly violated, as the joint probability of the edges  $X \rightarrow Y$  and  $Y \rightarrow X$  is non-zero as soon as both independently have non-zero probability.

This motivates that any distribution over parent sets resp. DAGs should (A) be able to represent a rich, multi-modal distribution over parent sets for each node, and (B) the joint distribution over parent sets of all nodes should be able to concentrate its support on acyclic graphs. Considering

these properties, we propose an expressive, yet tractable distribution over DAGs in the following.

To provide property (A), we propose to represent the distribution over parent sets for each node with a mixture of Multinoulli distributions parameterised by  $\phi_{\text{MN}} \in \mathbb{R}^{d \times K \times d}$ , i.e., for each node  $i$  the  $k$ -th component of the mixture has corresponding logits  $\phi_{\text{MN}}[i, k]$  and is a collection of  $d$  independent Bernoulli probabilities, indicating parenthood of all nodes  $j$  w.r.t. the sink node  $i$ . To provide the coupling between parent sets as required by property (B), we select the  $k$ -th Multinoulli mixture component by sampling from a mixture of categorical distributions with logits  $\phi_{\text{MOM}} \in \mathbb{R}^{M \times d \times K}$ , i.e., the  $m$ -th component of this mixture of mixtures contains for each sink node  $i$  a set of  $K$  mixture weights. We select the component of this top-level mixture by sampling from a categorical distribution according to mixture weights  $\phi_{\text{TLM}} \in \mathbb{R}^M$ . Finally, to model the dependence of the parent sets on the causal order  $L$  in  $p(\mathbf{Pa} | L, \phi)$ , we compute the logits  $\{\phi_{\text{MN}}, \phi_{\text{MOM}}, \phi_{\text{TLM}}\}$  using a differentiable function  $h_\theta(\cdot)$  (e.g., as in our case a simple feed-forward neural network) taking as input the permutation matrix  $Q^L$  induced by the causal order  $L$ . The expressiveness of the resulting distribution is determined by the richness of  $h(\cdot)$  and the number of mixture components  $M$  and  $K$ . We summarise the sampling procedure in Alg. 1.

### 3.1.3 Causal Order Inference

Similarly to § 3.1.2, the expectation w.r.t. causal orders in Eqs. (3.2) and (3.4) poses a hard combinatorial, as the number of permutations of  $d$  elements is  $d!$ . Thus, we aim to perform Monte Carlo estimation using a proposal distribution for causal orders. Following the considerations about proposal design regarding the parent set proposal, we illustrate potential pitfalls regarding distributions over causal orders. Consider any MEC including a chain graph. Consequently, the reverse chain graph must also be in the MEC, and thus, that the proposal over causal orders must be able to represent both chains with high probability.

Note that a simple parametrisation as in [Charpentier et al., 2022] is not able to represent the true posterior over causal orders in this case. Specifically, they sample orders using the Gumbel Top-k trick [Kool et al., 2019] using only  $d$  logits to represent a distribution of permutations over  $d$  elements. Now, to sample a chain graph and a reverse chain graph, one element is the root node in one case and must thus have the highest (perturbed) logit, and the leaf node in the other case where it must have the lowest (perturbed) logit, which is contradictory.

---

### Algorithm 2: Sample Causal Order

---

**Input:** Logit function  $g_\theta : \mathbb{R}^{d \times d} \mapsto (\mathbb{R}^d, \mathbb{R}^{d \times M \times d})$   
**Output:** Causal order  $L$  sampled from  $p(L | \theta)$   
 $U \leftarrow \mathbf{X}$  ▷ unassigned elements  
 $L \leftarrow \emptyset$  ▷ causal order  
 $k \leftarrow 1$  ▷ current layer index  
**repeat**  
     $\theta_{\text{CAT}} \leftarrow g(Q^{L_{<k}})$  ▷ compute logits  
     $L_k \sim \text{CAT}(L_k | \theta_{\text{CAT}}, U)$  ▷ sample next element  
     $L \leftarrow L \cup \{L_k\}$  ▷ update causal order  
     $U \leftarrow U \setminus L_k$  ▷ update unassigned  
     $k \leftarrow k + 1$   
**until**  $U \neq \emptyset$

---

In the following, we propose an expressive, auto-regressive proposal distribution

$$p(L | \theta) = p(L_1 | \theta) \cdot \prod_{k=2}^d p(L_k | L_{<k}, \theta) \quad (3.12)$$

for causal orders, that is amenable to gradient-based optimisation and avoids the shortcoming described above. The ordering of nodes naturally implies a sequential sampling procedure as listed in Alg. 2. In each step of the sampling procedure, we sample from  $p(L_k | L_{<k}, \theta)$  an element from the set of yet unassigned elements, conditional on all preceding elements from a categorical distribution  $p(L_k | L_{<k}, \theta)$ . To account for the dependence on preceding elements, we compute the logits of the categorical distribution using a differentiable function  $g_\theta(\cdot)$  (e.g., as in our case a simple feed-forward neural network) taking as input a suitable encoding of the so-far sampled order. We chose to encode these (sub-)orders using their induced permutation matrix  $Q^{L_{<k}}$  where we mask the rows corresponding to elements  $L_{\geq k}$  with zeros. To evaluate  $p(L_k | L_{<k}, \theta)$ , we compute the logits given the masked permutation matrix  $Q^{L_{<k}}$  and re-normalise them according to the elements in  $[L_{\geq k}]$  to get the probability of element  $L_k$  having been sampled at the  $k$ -th position in the order.

We again use the score-function estimator to estimate the gradient in Eq. (3.4) w.r.t.  $\theta$  as

$$\begin{aligned} \nabla_\theta \log p(\theta, \phi, \psi | \mathcal{D}) = & \quad (3.13) \\ \nabla_\theta \log p(\theta) + \mathbb{E}_{L | \theta} [\mathbb{E}_{\mathbf{Pa} | L, \phi} [w] \cdot \nabla_\theta p(L | \theta)] . \end{aligned}$$

with  $w$  as defined in Eq. (3.3).

### 3.1.4 Bringing it all together: Rao-Blackwellisation via Sequential Inference

Recall that we optimise our model by inferring MAP estimates of the parameter posterior by performing gradient as-

cent on  $\log p(\theta, \phi, \psi | \mathcal{D})$ . The standard approach of simultaneously updating all parameters in a single gradient step is prone to yield very noisy gradients:

1. The gradient w.r.t.  $\phi$  (parent set model) depends on  $\psi$  through the quality of the estimated the importance weights  $w$  in Eq. (3.11). Therefore, a bad estimate of  $\psi$  will result in poor estimates of the importance weights.
2. The gradient w.r.t.  $\theta$  (causal order model) additionally depends on  $\phi$  via the quality of the sampled parent sets in Eq. (3.13). Therefore, a bad estimate of  $\phi$  will lead to a poor proposal of parent sets that are not representative of the respective causal order.

To mitigate these issues, we propose a sequential, coordinate-descent style optimisation procedure. Whenever we sample a yet unseen parent set, we first optimise the associated GP hyper-parameters via MAP-Type II (see § 3.1.1), ensuring high-quality importance weight estimates.

When exhaustively enumerating the parent sets is possible, we get a low-variance gradient estimate for the causal order model in Eq. (3.13). Alternatively, when using the parent set proposal to approximately infer parent sets, we propose a two-stage approach. First, we approximate the expectation  $\mathbb{E}_{\mathbf{pa} | L, \phi} [w]$  in Eq. (3.13) with a single set of parents sets, specifically, with the set of maximal parent sets consistent with the causal order (i.e., the resulting DAG would be the adjacency mask induced by  $L$ ) and optimise the causal order model independently of the parent set model. Second, we leave  $\theta$  fixed and optimise the parent set model via Eq. (3.11). We show the effectiveness of this sequential optimisation procedure in an ablation study in Appx. C.

## 4 RELATED WORK

The Bayesian causal inference problem that we focus on in this paper was recently motivated by [Toth et al., 2022], but dates back in the simpler form of Bayesian structure inference [Heckerman, 1995, Heckerman et al., 1997].

Utilising (causal) orders is an well established approach in the MCMC-based Bayesian structure learning community. The combinatorial space of orders is significantly smaller than the combinatorial space of DAGs, which serves MCMC methods to better explore the posterior space of DAGs [Koller and Friedman, 2003, Koivisto and Sood, 2004, Teyssier and Koller, 2012, Niinimäki et al., 2016, Vinikka et al., 2020]. Moreover, the restriction of the maximum size of any parent set in the DAG allows for the exhaustive enumeration of all parent sets in polynomial time. However, MCMC inference comes with its own set of challenges, and none of these works can handle non-linear mechanism models.

Besides sampling based inference, introducing order structure also leads to exact optimization schemes [Cussens, 2010, De Campos and Ji, 2011, Peharz and Pernkopf, 2012].

After the advent of differentiable DAG structure learning methods [Zheng et al., 2018, Yu et al., 2019, Brouillard et al., 2020, Lachapelle et al., 2020, Lorch et al., 2021], inference via orders recently resurfaced in the causal structure learning community, mainly as a vehicle to sample DAGs without the need of utilising soft acyclicity constraints during optimisation [Cundy et al., 2021, Charpentier et al., 2022, Annadani et al., 2023]. In contrast to these works, although we use gradient-based optimisation to learn a distribution over causal orders, we mainly utilise causal orders to Rao-Blackwellise our inference procedure by exhaustive parent set enumeration.

## 5 EXPERIMENTS

### 5.1 SETUP

We briefly summarise our experimental setup in the following. Additional results and ablations are provided in Appx. C. We provide our code as a supplementary material.

**Data.** We generate ground truth SCMs with  $d = 20$  endogenous variables with graph structures sampled from the commonly used Erdős-Rényi (ER) [Erdős and Rényi, 1959] and scale-free (SF) [Barabási and Albert, 1999] models (cf. [Lorch et al., 2021, Charpentier et al., 2022, Annadani et al., 2023, Toth et al., 2022]). We evaluate our method both on linear and on non-linear additive noise models. For each ground truth SCM, we sample a fixed set of 100 training, and 200 test samples from the observational distribution. This emulates the setting of significant uncertainty relevant to the Bayesian inference scenario. Reischach et al. [2021] argue, that the causal order may strongly correlate with increasing marginal variance in simulated data, and therefore, benchmarks may be easy to game by exploiting this property. As this may be especially relevant to order-based inference methods, we follow their recommendation and normalise the training data for each endogenous variable to zero mean and unit variance.

**Metrics.** As is custom, we report the *expected structural Hamming distance* (ESHD), as well as the *area under the receiver operating characteristic* (AUROC) and the *area under the precision recall curve* (AUPRC) w.r.t. posterior edge prediction. Following Annadani et al. [2023], we also report the F1 score, and, to provide additional insight into the methods strengths and weaknesses, we also report the *true positive rate* (TPR) and *true negative rate* (TNR) for the edge prediction task. Finally, to evaluate the quality of

the inferred causal mechanisms, we report the *expected relative root-mean-square error* (RRMSE) on the test set. We do **not** report the log-likelihood on the test data as is usually done, because the evaluated methods implement different noise models and approximate inference schemes, which leads to the (marginal) log-likelihoods being uncalibrated and thus incomparable (cf. [Murphy, 2023][Sec. 7.5] and references therein).

**Baselines.** We compare our two model variants, i.e., exhaustive enumeration of parent sets with maximum size  $K = 2$  (COM-EX-GP) vs. approximate gradient-based parent set inference (COM-PSM-GP), to three recent structure learning methods. First, we compare against DIBS, proposed by Lorch et al. [2021], which implements differentiable Bayesian graph learning using a soft acyclicity constraint in line with Zheng et al. [2018], Yu et al. [2019]. Second, we compare against DDS, proposed by Charpentier et al. [2022], which builds upon the permutation-based approach of Cundy et al. [2021] and utilises differentiable permutation sampling and variational inference (VI) to infer a posterior over DAGs. Third, we compare against BayesDAG, proposed by Annadani et al. [2023], which utilises a mixture of MCMC to infer permutations and mechanism parameters, and VI to infer DAG edges given the permutations. DDS and BayesDAG both utilise causal orders for structure learning.

## 5.2 RESULTS

Our results in Tab. 1 show, that our COM-EX-GP method consistently and substantially outperforms the baselines on all metrics in all scenarios, except for TPR (see discussion below). This is to be expected on scale-free graphs, where the restriction to parent sets of maximum size  $K = 2$  conforms with the structural properties of the ground-truth causal graphs. Interestingly, COM-EX-GP also delivers strong results on SCMs with Erdős-Rényi graph structures, although the assumption on the parent set sizes is clearly violated. Given the consistently high TNR demonstrates that our models infer very well which edges are not present and give high scores to sub-graphs of the true graph.

Our second model variant, COM-PSM-GP, achieves competitive scores especially in the linear scenario. We conjecture that, as in the linear case the true causal graph is not identifiable, using an expressive proposal distribution over parent sets (see § 3.1.2) is paramount. In contrast, in the non-linear case the true graph is identifiable and thus, an expressive parent set proposal may not be necessary or even detrimental, as it may be harder to optimise. Notably, except for the Erdős-Rényi linear case, this model variant has a rather high ESHD joined by a high expected number of edges. Most likely, using an explicit, tuned sparsity regu-

larising mechanism as used by DDS and BayesDAG would improve performance.

Among the baselines, BayesDAG performs best on most metrics in the majority of cases and represents a strong baseline method. DDS suffers from a high ESHD and predicts significantly more edges in expectation than all other methods. This is reflected by a high TPR and a low TNR, i.e., DDS predicts very dense graphs. Unfortunately, we could not find suitable hyper-parameters to regularise the sparsity, and similar behaviour was reported by Annadani et al. [2023][App. G, Fig. 4]. We hypothesise that (i) the posterior over causal orders fails to capture the true posterior for reasons explained in § 3.1.3, and (ii) the missing coupling between causal orders and edge probabilities. DIBS obtains higher TNR than TPR and a rather low expected number of edges in comparison with the other methods. We conjecture that, although we did not use an explicit sparsity regulariser, the optimisation involving the soft acyclicity constraint acts as an implicit sparsity regulariser, as sparse graphs are more likely to have a lower cyclicity score than denser ones.

## 6 DISCUSSION

Instead of attempting to directly infer a posterior over SCMs, we shift the Bayesian causal inference problem to inferring high-quality proposal densities amenable to gradient-based optimisation, which we use to compute Monte-Carlo estimates via importance sampling. We stress the importance of Rao-Blackwellising the inference procedure and show its effectiveness on simulated benchmarks. Specifically, for the case of (non-)linear additive noise models, we improve upon a set of state-of-the-art baseline methods. Some limitations and potential improvements are described in the following.

**Modelling Mechanisms.** The main driver of complexity is the exact inference using GPs, which grows with  $N^3$  in the number of available data points. Although we used only CPUs for running our experiments, scalable GPU inference techniques for GPs were proposed by Gardner et al. [2018], Pleiss et al. [2018]. Conceptually, our framework is flexible and modular, allowing to use alternative mechanism models like normalising flows as in Brouillard et al. [2020], Pawłowski et al. [2020]. Lastly, given our sequential inference procedure, the training of the mechanisms could be parallelised.

**Parent Set Inference.** A second driver of computational complexity is the exhaustive enumeration of parent sets. The number of parent sets with bounded size  $K$  grows polynomially with  $O(d^K)$ , which may be prohibitive on larger problem instances. Note, however, that the necessary weights can be pre-computed in parallel. An interesting ex-

Table 1: Experimental results on simulated (non-)linear ground truth models with 20 nodes and different DAG structures. We report means and 95% confidence intervals (CIs) across 20 different ground truth models. Best values are bold-faced. As the true graph is not identifiable in the linear scenario, the reported structure learning metrics are computed w.r.t. the skeleton of the true DAG.

| Model             | #Edges  | ↓ ESHD        | ↑ AUROC            | ↑ AUPRC            | ↑ TPR              | ↑ TNR              | ↑ F1               | ↓ RRMSE            |
|-------------------|---------|---------------|--------------------|--------------------|--------------------|--------------------|--------------------|--------------------|
| DDS               | 157 ± 7 | 127 ± 5       | 0.80 ± 0.03        | 0.57 ± 0.05        | <b>0.90 ± 0.03</b> | 0.19 ± 0.04        | 0.35 ± 0.02        | 1.04 ± 0.03        |
| DIBS              | 21 ± 4  | 39 ± 4        | 0.69 ± 0.02        | 0.45 ± 0.03        | 0.27 ± 0.05        | 0.93 ± 0.02        | 0.34 ± 0.05        | 1.44 ± 0.05        |
| BayesDAG          | 38 ± 2  | 39 ± 3        | 0.74 ± 0.03        | 0.56 ± 0.05        | 0.49 ± 0.03        | 0.87 ± 0.01        | 0.49 ± 0.03        | 0.91 ± 0.03        |
| COM-EX-GP (ours)  | 26 ± 1  | <b>22 ± 2</b> | <b>0.82 ± 0.03</b> | <b>0.73 ± 0.03</b> | 0.55 ± 0.03        | <b>0.97 ± 0.01</b> | <b>0.66 ± 0.03</b> | <b>0.21 ± 0.00</b> |
| COM-PSM-GP (ours) | 89 ± 6  | 72 ± 4        | 0.66 ± 0.02        | 0.54 ± 0.02        | 0.72 ± 0.04        | 0.60 ± 0.03        | 0.43 ± 0.02        | 1.07 ± 0.06        |

(a) Erdős-Rényi Nonlinear.

| Model             | #Edges  | ↓ ESHD        | ↑ AUROC            | ↑ AUPRC            | ↑ TPR              | ↑ TNR              | ↑ F1               | ↓ RRMSE            |
|-------------------|---------|---------------|--------------------|--------------------|--------------------|--------------------|--------------------|--------------------|
| DDS               | 168 ± 5 | 137 ± 4       | 0.79 ± 0.03        | 0.54 ± 0.05        | <b>0.93 ± 0.02</b> | 0.13 ± 0.03        | 0.33 ± 0.00        | 1.01 ± 0.04        |
| DIBS              | 35 ± 5  | 42 ± 4        | 0.71 ± 0.02        | 0.46 ± 0.04        | 0.40 ± 0.06        | 0.87 ± 0.02        | 0.40 ± 0.05        | 1.42 ± 0.06        |
| BayesDAG          | 65 ± 2  | 48 ± 2        | 0.82 ± 0.03        | 0.61 ± 0.04        | 0.73 ± 0.03        | 0.75 ± 0.01        | 0.52 ± 0.02        | 0.88 ± 0.03        |
| COM-EX-GP (ours)  | 32 ± 1  | <b>13 ± 2</b> | <b>0.93 ± 0.02</b> | <b>0.87 ± 0.04</b> | 0.77 ± 0.03        | <b>0.97 ± 0.01</b> | <b>0.81 ± 0.03</b> | <b>0.20 ± 0.00</b> |
| COM-PSM-GP (ours) | 88 ± 4  | 68 ± 4        | 0.69 ± 0.02        | 0.55 ± 0.02        | 0.77 ± 0.03        | 0.61 ± 0.03        | 0.45 ± 0.02        | 1.04 ± 0.04        |

(b) Scale-free Nonlinear.

| Model             | #Edges  | ↓ ESHD        | ↑ AUROC            | ↑ AUPRC            | ↑ TPR              | ↑ TNR              | ↑ F1               | ↓ RRMSE            |
|-------------------|---------|---------------|--------------------|--------------------|--------------------|--------------------|--------------------|--------------------|
| DDS               | 156 ± 5 | 126 ± 3       | 0.68 ± 0.02        | 0.38 ± 0.03        | <b>0.88 ± 0.03</b> | 0.19 ± 0.03        | 0.35 ± 0.02        | 0.60 ± 0.04        |
| DIBS              | 39 ± 6  | 56 ± 6        | 0.58 ± 0.03        | 0.37 ± 0.03        | 0.29 ± 0.03        | 0.82 ± 0.04        | 0.29 ± 0.03        | 0.50 ± 0.07        |
| BayesDAG          | 38 ± 3  | 48 ± 5        | 0.65 ± 0.04        | 0.41 ± 0.03        | 0.38 ± 0.04        | 0.85 ± 0.02        | 0.38 ± 0.03        | 0.30 ± 0.03        |
| COM-EX-GP (ours)  | 31 ± 2  | <b>40 ± 4</b> | 0.68 ± 0.03        | 0.44 ± 0.04        | 0.40 ± 0.03        | <b>0.90 ± 0.01</b> | <b>0.44 ± 0.03</b> | <b>0.17 ± 0.00</b> |
| COM-PSM-GP (ours) | 31 ± 2  | <b>40 ± 4</b> | <b>0.69 ± 0.03</b> | <b>0.45 ± 0.03</b> | 0.38 ± 0.04        | 0.89 ± 0.01        | 0.43 ± 0.04        | <b>0.17 ± 0.00</b> |

(c) Erdős-Rényi Linear.

| Model             | #Edges  | ↓ ESHD        | ↑ AUROC            | ↑ AUPRC            | ↑ TPR              | ↑ TNR              | ↑ F1               | ↓ RRMSE            |
|-------------------|---------|---------------|--------------------|--------------------|--------------------|--------------------|--------------------|--------------------|
| DDS               | 163 ± 2 | 136 ± 1       | 0.59 ± 0.04        | 0.29 ± 0.04        | <b>0.88 ± 0.01</b> | 0.15 ± 0.01        | 0.32 ± 0.00        | 0.35 ± 0.04        |
| DIBS              | 42 ± 4  | 60 ± 4        | 0.53 ± 0.03        | 0.29 ± 0.03        | 0.25 ± 0.04        | 0.79 ± 0.02        | 0.23 ± 0.03        | 0.22 ± 0.05        |
| BayesDAG          | 36 ± 3  | 55 ± 2        | 0.54 ± 0.03        | 0.25 ± 0.03        | 0.23 ± 0.04        | 0.82 ± 0.01        | 0.23 ± 0.04        | 0.20 ± 0.02        |
| COM-EX-GP (ours)  | 34 ± 1  | <b>47 ± 3</b> | <b>0.61 ± 0.03</b> | 0.33 ± 0.04        | 0.32 ± 0.04        | <b>0.85 ± 0.01</b> | <b>0.33 ± 0.04</b> | <b>0.16 ± 0.00</b> |
| COM-PSM-GP (ours) | 86 ± 8  | 87 ± 6        | 0.52 ± 0.02        | <b>0.40 ± 0.02</b> | 0.49 ± 0.04        | 0.56 ± 0.04        | 0.29 ± 0.01        | 0.21 ± 0.05        |

(d) Scale-free Linear.

tension of our work would be to use e.g.  $K=2$  as approximation to learn a good proposal distribution over causal orders, and then to subsequently infer unrestricted parent sets with our proposed parent set model.

**Alternative Inference Techniques.** We employ the score-function estimator to compute the gradient estimates for the causal order and parent set models. Although this estimator is known to suffer from high variance, it is unbiased and we achieve good results using a simple exponential moving average baseline. Furthermore, it would be interesting to see how a variational inference approach would fare when incorporating our expressive proposal distributions as variational distributions.

**Impact Statement.** This paper presents work whose goal is to advance the field of Machine Learning. There are many potential societal consequences of our work, none which we feel must be specifically highlighted here.

## Acknowledgements

The computational results presented have in part been achieved using the Vienna Scientific Cluster (VSC).

## References

Yashas Annadani, Nick Pawlowski, Joel Jennings, Stefan Bauer, Cheng Zhang, and Wenbo Gong. Bayes{DAG}:



- Gradient-Based Posterior Inference for Causal Discovery. In *Thirty-seventh Conference on Neural Information Processing Systems*, 2023.
- Albert-László Barabási and Réka Albert. Emergence of scaling in random networks. *Science*, 286, 1999.
- Philippe Brouillard, Sébastien Lachapelle, Alexandre Lacoste, Simon Lacoste-Julien, and Alexandre Drouin. Differentiable Causal Discovery from Interventional Data. In H Larochelle, M Ranzato, R Hadsell, M F Balcan, and H Lin, editors, *Advances in Neural Information Processing Systems*. Curran Associates, Inc., 2020.
- Bertrand Charpentier, Simon Kibler, and Stephan Günnemann. Differentiable {DAG} Sampling. In *International Conference on Learning Representations*, 2022.
- Chris Cundy, Aditya Grover, and Stefano Ermon. BCD Nets: Scalable Variational Approaches for Bayesian Causal Discovery. In *Thirty-Fifth Conference on Neural Information Processing Systems*, 2021.
- James Cussens. Maximum likelihood pedigree reconstruction using integer programming. In *WCB@ ICLP*, pages 8–19, 2010.
- Cassio P De Campos and Qiang Ji. Efficient structure learning of bayesian networks using constraints. *The Journal of Machine Learning Research*, 12:663–689, 2011.
- P. Erdős and A. Rényi. On random graphs i. *Publicationes Mathematicae Debrecen*, 6:290, 1959.
- Jacob Gardner, Geoff Pleiss, Kilian Q Weinberger, David Bindel, and Andrew G Wilson. Gpytorch: Blackbox matrix-matrix gaussian process inference with gpu acceleration. In S. Bengio, H. Wallach, H. Larochelle, K. Grauman, N. Cesa-Bianchi, and R. Garnett, editors, *Advances in Neural Information Processing Systems*. Curran Associates, Inc., 2018.
- Paula Gradu, Tijana Zrnic, Yixin Wang, and Michael I. Jordan. Valid Inference after Causal Discovery. *arXiv:2208.05949*, 2022.
- David Heckerman. A bayesian approach to learning causal networks. In *Proceedings of Eleventh Conference on Uncertainty in Artificial Intelligence*. Morgan Kaufmann, 1995.
- David Heckerman, Christopher Meek, and Gregory Cooper. A Bayesian Approach to Causal Discovery. *Computation, Causation, and Discovery*, 1997.
- Mikko Koivisto and Kismat Sood. Exact Bayesian structure discovery in Bayesian networks. *Journal of Machine Learning Research*, 2004.
- D. Koller and N. Friedman. Being Bayesian about network structure. A Bayesian approach to structure discovery in Bayesian networks. *Machine Learning*, 2003.
- Wouter Kool, Herke Van Hoof, and Max Welling. Stochastic Beams and Where To Find Them: The {G}umbel-Top-k Trick for Sampling Sequences Without Replacement. In Kamalika Chaudhuri and Ruslan Salakhutdinov, editors, *Proceedings of the 36th International Conference on Machine Learning*, volume 97. PMLR, 2019. URL <https://proceedings.mlr.press/v97/kool19a.html>.
- Sébastien Lachapelle, Philippe Brouillard, Tristan Deleu, and Simon Lacoste-Julien. Gradient-Based Neural DAG Learning. In *International Conference on Learning Representations*, 2020.
- Lars Lorch, Jonas Rothfuss, Bernhard Schölkopf, and Andreas Krause. DiBS: Differentiable Bayesian Structure Learning. *Advances in Neural Information Processing Systems*, 2021.
- Kevin P. Murphy. *Probabilistic Machine Learning: An introduction*. MIT Press, 2021.
- Kevin P. Murphy. *Probabilistic Machine Learning: Advanced Topics*. MIT Press, 2023.
- Teppo Niinimäki, Pekka Parviainen, and Mikko Koivisto. Structure Discovery in Bayesian Networks by Sampling Partial Orders. *Journal of Machine Learning Research*, 2016.
- OEIS Foundation Inc. Number of acyclic digraphs (or dags) with n labeled nodes, 2024. Entry A003024 in The On-Line Encyclopedia of Integer Sequences, <https://oeis.org/A003024>.
- Nick Pawlowski, Daniel C Castro, and Ben Glocker. Deep Structural Causal Models for Tractable Counterfactual Inference. In *Advances in Neural Information Processing Systems*, 2020.
- Judea Pearl. *Causality*. Cambridge University Press, 2009. ISBN 9780511803161.
- Robert Peharz and Franz Pernkopf. Exact maximum margin structure learning of bayesian networks. *arXiv preprint arXiv:1206.6431*, 2012.
- Geoff Pleiss, Jacob Gardner, Kilian Weinberger, and Andrew Gordon Wilson. Constant-time predictive distributions for Gaussian processes. In Jennifer Dy and Andreas Krause, editors, *Proceedings of the 35th International Conference on Machine Learning*, Proceedings of Machine Learning Research. PMLR, 2018.

Alexander G. Reisach, Christof Seiler, and Sebastian Weichwald. Beware of the Simulated DAG! Causal Discovery Benchmarks May Be Easy To Game. In M. Ranzato Vaughan, A. Beygelzimer, Y. Dauphin, P.S. Liang, and J. Wortman, editors, *Advances in Neural Information Processing Systems*. Curran Associates, Inc., 2021.

Marc Teyssier and Daphne Koller. Ordering-Based Search: A Simple and Effective Algorithm for Learning Bayesian Networks. *Proceedings of the 21st Conference on Uncertainty in Artificial Intelligence, UAI 2005*, 2012.

Christian Toth, Lars Lorch, Christian Knoll, Andreas Krause, Franz Pernkopf, Robert Peharz, and Julius von Kügelgen. Active Bayesian Causal Inference. In S Koyejo, S Mohamed, A Agarwal, D Belgrave, K Cho, and A Oh, editors, *Advances in Neural Information Processing Systems*. Curran Associates, Inc., 2022.

Jussi Viinikka, Antti Hyttinen, Johan Pensar, and Mikko Koivisto. Towards Scalable Bayesian Learning of Causal DAGs. In H Larochelle, M Ranzato, R Hadsell, M F Balcan, and H Lin, editors, *Advances in Neural Information Processing Systems*. Curran Associates, Inc., 2020.

Yue Yu, Jie Chen, Tian Gao, and Mo Yu. DAG-GNN: DAG Structure Learning with Graph Neural Networks. In Kamalika Chaudhuri and Ruslan Salakhutdinov, editors, *Proceedings of the 36th International Conference on Machine Learning*, Proceedings of Machine Learning Research. PMLR, 2019.

Xun Zheng, Bryon Aragam, Pradeep K Ravikumar, and Eric P Xing. DAGs with NO TEARS: Continuous Optimization for Structure Learning. In S Bengio, H Wallach, H Larochelle, K Grauman, N Cesa-Bianchi, and R Garnett, editors, *Advances in Neural Information Processing Systems 31*. Curran Associates, Inc., 2018.

---

# Rao-Blackwellising Bayesian Causal Inference (Supplementary Material)

---

Christian Toth<sup>1</sup>

Christian Knoll<sup>1,2</sup>

Franz Pernkopf<sup>1</sup>

Robert Peharz<sup>1</sup>

<sup>1</sup>Graz University of Technology

<sup>2</sup>Levata GmbH

## A PROOFS AND DERIVATIONS

### A.1 DERIVATION OF THE POSTERIOR EXPECTATION W.R.T. SCMS

In the following, we derive the expectation w.r.t. SCMs in Eq. (3.2) and the corresponding importance weights in Eq. (3.3).

$$\begin{aligned}
\mathbb{E}_{\mathcal{M}|\mathcal{D}}[Y(\mathcal{M})] &= \mathbb{E}_{G,\mathbf{f},\psi|\mathcal{D}}[Y(\mathcal{M})] \\
&= \mathbb{E}_{\boldsymbol{\theta},\phi,\psi|\mathcal{D}}[\mathbb{E}_{G,\mathbf{f}|\boldsymbol{\theta},\phi,\psi,\mathcal{D}}[Y(\mathcal{M})]] \\
&= \mathbb{E}_{\boldsymbol{\theta},\phi,\psi|\mathcal{D}}[\mathbb{E}_{G|\boldsymbol{\theta},\phi,\psi,\mathcal{D}}[\mathbb{E}_{\mathbf{f}|\psi,\mathcal{D}}[Y(\mathcal{M})]]] \\
&= \mathbb{E}_{\boldsymbol{\theta},\phi,\psi|\mathcal{D}}\left[\mathbb{E}_{G|\boldsymbol{\theta},\phi}\left[\frac{p(\boldsymbol{\psi},\mathcal{D}|G)}{p(\boldsymbol{\psi},\mathcal{D}|\boldsymbol{\theta},\phi)}\mathbb{E}_{\mathbf{f}|\psi,\mathcal{D}}[Y(\mathcal{M})]\right]\right] \\
&= \mathbb{E}_{\boldsymbol{\theta},\phi,\psi|\mathcal{D}}[\mathbb{E}_{L|\boldsymbol{\theta}}[\mathbb{E}_{\mathbf{Pa}|L,\phi}[w \cdot \mathbb{E}_{\mathbf{f}|\psi,\mathcal{D}}[Y(\mathcal{M})]]]]
\end{aligned}$$

with

$$\begin{aligned}
w &:= \frac{p(\boldsymbol{\psi},\mathcal{D}|G)}{p(\boldsymbol{\psi},\mathcal{D}|\boldsymbol{\theta},\phi)} \\
&= \frac{p(\boldsymbol{\psi},\mathcal{D}|G)}{\mathbb{E}_{L'|\boldsymbol{\theta}}[\mathbb{E}_{\mathbf{Pa}'|L',\phi}[p(\boldsymbol{\psi},\mathcal{D}|G)]]} \\
&= \frac{p(\mathcal{D}|\boldsymbol{\psi},G) \cdot p(\boldsymbol{\psi}|G)}{\mathbb{E}_{L'|\boldsymbol{\theta}}[\mathbb{E}_{\mathbf{Pa}'|L',\phi}[p(\mathcal{D}|\boldsymbol{\psi},G) \cdot p(\boldsymbol{\psi}|G)]]}.
\end{aligned}$$

### A.2 DERIVATION OF THE GRADIENT ESTIMATORS

In the following, we derive the gradient estimators in Eqs. (3.4), (3.11) and (3.13). We denote by  $\nabla = \nabla_{\boldsymbol{\theta},\phi,\psi}$  to avoid clutter.

The general posterior gradient reads as follows.

$$\begin{aligned}
\nabla \log p(\boldsymbol{\theta}, \phi, \boldsymbol{\psi} | \mathcal{D}) &= \nabla \log \frac{p(\mathcal{D} | \boldsymbol{\theta}, \phi, \boldsymbol{\psi}) \cdot p(\boldsymbol{\theta}, \phi, \boldsymbol{\psi})}{p(\mathcal{D})} \\
&= \nabla \log p(\boldsymbol{\theta}, \phi, \boldsymbol{\psi}) + \nabla \log p(\mathcal{D} | \boldsymbol{\theta}, \phi, \boldsymbol{\psi}) \\
&= \nabla \log p(\boldsymbol{\theta}, \phi) + \nabla \log p(\mathcal{D}, \boldsymbol{\psi} | \boldsymbol{\theta}, \phi) \\
&= \nabla \log p(\boldsymbol{\theta}, \phi) + \nabla \log \mathbb{E}_{L|\boldsymbol{\theta}}[p(\mathcal{D}, \boldsymbol{\psi} | L, \phi)] \\
&= \nabla \log p(\boldsymbol{\theta}, \phi) + \nabla \log \mathbb{E}_{L|\boldsymbol{\theta}}[\mathbb{E}_{\mathbf{Pa}|L,\phi}[p(\mathcal{D}, \boldsymbol{\psi} | G = \mathbf{Pa} \odot M^L)]]
\end{aligned}$$

Using this as starting point for the partial gradients, we get

$$\begin{aligned}
\nabla_{\phi} \log p(\boldsymbol{\theta}, \phi, \boldsymbol{\psi} | \mathcal{D}) &= \nabla_{\phi} \log p(\boldsymbol{\theta}, \phi) + \nabla_{\phi} \log \mathbb{E}_{L|\boldsymbol{\theta}}[\mathbb{E}_{\mathbf{Pa}|L,\phi}[p(\mathcal{D}, \boldsymbol{\psi} | G = \mathbf{Pa} \odot M^L)]] \\
&= \nabla_{\phi} \log p(\phi) + \nabla_{\phi} \log \mathbb{E}_{L|\boldsymbol{\theta}}[\mathbb{E}_{\mathbf{Pa}|L,\phi}[p(\mathcal{D}, \boldsymbol{\psi} | G = \mathbf{Pa} \odot M^L)]] \\
&= \nabla_{\phi} \log p(\phi) + \mathbb{E}_{L|\boldsymbol{\theta}}\left[\frac{\nabla_{\phi} \mathbb{E}_{\mathbf{Pa}|L,\phi}[p(\mathcal{D}, \boldsymbol{\psi} | G = \mathbf{Pa} \odot M^L)]}{\mathbb{E}_{L'|\boldsymbol{\theta}}[\mathbb{E}_{\mathbf{Pa}'|L',\phi}[p(\mathcal{D}, \boldsymbol{\psi} | G = \mathbf{Pa}' \odot M^{L'})]]}\right]
\end{aligned}$$

and using  $\nabla_{\phi} p(\mathbf{Pa} | L, \phi) = p(\mathbf{Pa} | L, \phi) \cdot \nabla_{\phi} \log p(\mathbf{Pa} | L, \phi)$

$$\begin{aligned}
&= \nabla_{\phi} \log p(\phi) + \mathbb{E}_{L|\boldsymbol{\theta}}\left[\frac{\mathbb{E}_{\mathbf{Pa}|L,\phi}[p(\mathcal{D}, \boldsymbol{\psi} | G = \mathbf{Pa} \odot M^L) \cdot \nabla_{\phi} \log p(G | L, \phi)]}{\mathbb{E}_{L'|\boldsymbol{\theta}}[\mathbb{E}_{\mathbf{Pa}'|L',\phi}[p(\mathcal{D}, \boldsymbol{\psi} | G = \mathbf{Pa}' \odot M^{L'})]]}\right] \\
&= \nabla_{\phi} \log p(\phi) + \mathbb{E}_{L|\boldsymbol{\theta}}[w \cdot \nabla_{\phi} \log p(G | L, \phi)].
\end{aligned}$$

The derivation for the gradient in Eq. (3.13) follows by analogy.

### A.3 PROOFS REGARDING EXHAUSTIVE PARENT SET ENUMERATION

#### Proof of Prop. 3.1

*Proof.*

$$\mathbb{E}_{G|L} [w(G) \cdot Y(G)] = \sum_G p(G|L) \cdot w(G) \cdot Y(G)$$

Since we assume that  $w(G)$  and  $Y(G)$  factorise over the parent sets, we have

$$= \sum_G \prod_i p(\mathbf{Pa}_i^G | L) \cdot w_i(\mathbf{Pa}_i^G) \cdot Y_i(\mathbf{Pa}_i^G)$$

The sum over all graphs can be represented as sum over all combinations of possible parent sets to get

$$\begin{aligned} &= \sum_{\mathbf{Pa}_1} \sum_{\mathbf{Pa}_2} \cdots \sum_{\mathbf{Pa}_d} \prod_i p(\mathbf{Pa}_i | L) \cdot w_i(\mathbf{Pa}_i) \cdot Y_i(\mathbf{Pa}_i) \\ &= \sum_{\mathbf{Pa}_1} p(\mathbf{Pa}_1 | L) \cdot w_1(\mathbf{Pa}_1) \cdot Y_1(\mathbf{Pa}_1) \sum_{\mathbf{Pa}_2} p(\mathbf{Pa}_2 | L) \cdot w_2(\mathbf{Pa}_2) \cdot Y_2(\mathbf{Pa}_2) \cdots \end{aligned}$$

Since each summation over parent sets is independent of the others, we get the final result

$$= \prod_i \sum_{\mathbf{Pa}_i} p(\mathbf{Pa}_i | L) \cdot w_i(\mathbf{Pa}_i) \cdot Y_i(\mathbf{Pa}_i)$$

□

#### Proof of Prop. 3.2

*Proof.*

$$\begin{aligned} \mathbb{E}_{G|L} [w(G) \cdot Y(G)] \\ &= \sum_G p(G|L) \cdot w(G) \cdot Y(G) \end{aligned}$$

Since we assume that  $w(G)$  factorises and  $Y(G)$  sums over the parent sets, we have

$$= \sum_G \prod_i p(\mathbf{Pa}_i^G | L) \cdot w_i(\mathbf{Pa}_i^G) \cdot \sum_j Y_j(\mathbf{Pa}_j^G)$$

The sum over all graphs can be represented as sum over all combinations of possible parent sets to get

$$\begin{aligned} &= \sum_{\mathbf{Pa}_1} \sum_{\mathbf{Pa}_2} \cdots \sum_{\mathbf{Pa}_d} \prod_i p(\mathbf{Pa}_i | L) \cdot w_i(\mathbf{Pa}_i) \cdot \sum_j Y_j(\mathbf{Pa}_j) \\ &= \sum_{\mathbf{Pa}_1} \sum_{\mathbf{Pa}_2} \cdots \sum_{\mathbf{Pa}_d} \cdot \sum_j Y_j(\mathbf{Pa}_j) \prod_i p(\mathbf{Pa}_i | L) \cdot w_i(\mathbf{Pa}_i) \\ &= \sum_{\mathbf{Pa}_1} \sum_{\mathbf{Pa}_2} \cdots \sum_{\mathbf{Pa}_d} Y_1(\mathbf{Pa}_1) \prod_i p(\mathbf{Pa}_i | L) \cdot w_i(\mathbf{Pa}_i) + \sum_{\mathbf{Pa}_1} \sum_{\mathbf{Pa}_2} \cdots \sum_{\mathbf{Pa}_d} \sum_{j=2}^d \cdots \\ &= \sum_{\mathbf{Pa}_1} Y_1(\mathbf{Pa}_1) \cdot p(\mathbf{Pa}_1 | L) \cdot w_1(\mathbf{Pa}_1) \sum_{\mathbf{Pa}_2} p(\mathbf{Pa}_2 | L) \cdot w_2(\mathbf{Pa}_2) \cdots + \sum_{\mathbf{Pa}_1} \sum_{\mathbf{Pa}_2} \cdots \sum_{\mathbf{Pa}_d} \sum_{j=2}^d \cdots \end{aligned}$$

By abbreviating  $\alpha_j(L) = \sum_{\mathbf{pa}_i} p(\mathbf{pa}_i, L) w_i(\mathbf{pa}_i)$  we get

$$= \sum_{\mathbf{Pa}_1} Y_1(\mathbf{Pa}_1) \cdot p(\mathbf{Pa}_1 | L) \cdot w_1(\mathbf{Pa}_1) \cdot \prod_{j \neq 1} \alpha_j(L) + \sum_{\mathbf{Pa}_1} \sum_{\mathbf{Pa}_2} \cdots \sum_{\mathbf{Pa}_d} \sum_{j=2}^d Y_j(\mathbf{Pa}_j) \prod_i p(\mathbf{Pa}_i | L) \cdot w_i(\mathbf{Pa}_i)$$

By repeating this procedure for the remaining summands  $j$ , we get the final result

$$= \sum_i \left( \prod_{j \neq i} \alpha_j(L) \right) \cdot \sum_{\mathbf{Pa}_i} p(\mathbf{pa}_i | L) \cdot w_i(\mathbf{pa}_i) \cdot Y_i(\mathbf{Pa}_i)$$

□

## B EXPERIMENTAL SETUP

### B.1 SIMULATED DATA.

We follow the setup of [Lorch et al. \[2021\]](#), [Toth et al. \[2022\]](#) and generate scale-free and Erdős-Rényi graphs with an expected degree of 2.

### B.2 EVALUATION METRICS

Our evaluation metrics for edge prediction, i.e., AUROC, AUPRC, TPR, TNR and F1 are standard classification metrics as described e.g. by [Murphy \[2021\]](#). We computed the RRMSE on held-out observational test data

$$\mathcal{D}^{\text{TEST}} = \{\mathbf{x}^n \stackrel{\text{i.i.d.}}{\sim} p(\mathbf{X} | \mathcal{M}^*)\}_{n=1}^{N_T}$$

sampled from the true SCM  $\mathcal{M}^*$  as

$$\text{RRMSE} = \mathbb{E}_{\mathcal{M} | \mathcal{D}} \left[ \frac{1}{d} \sum_i \frac{\|\hat{\mathbf{x}}_i - \mathbf{x}_i\|_2}{\|\mathbf{x}_i\|_2} \right] \quad (\text{B.1})$$

where

$$\mathbf{x}_i = (x_1^n, x_2^n, \dots, x_3^n)^T$$

denotes the vector of test samples for node  $i$ , and

$$\hat{\mathbf{x}}_i = (\hat{x}_1^n, \hat{x}_2^n, \dots, \hat{x}_3^n)^T$$

denotes the vector of model predictions  $\hat{x}_1^n = f_i(\mathbf{pa}_i^G)$  for node  $i$  given a posterior SCM  $\mathcal{M} = (G, \mathbf{f}, \psi)$ .

### B.3 SIMULATION PARAMETERS

If not stated otherwise, we use a feed-forward neural network  $g_\theta$  with a single hidden layer of 30 neurons and ReLU activation function for our autoregressive causal order model. For our parent set model, we use  $M = K = 10$  mixture components and a feed-forward neural network  $h_\phi$  with a single hidden layer of 30 neurons and ReLU activation function. We train GPs in batches of 20 for a maximum of 100 steps and RMSprop optimiser with learning rate 0.02. For the estimation of gradients and scores, we sample 100 causal orders and 10 parent sets conditional on each sampled order. We train the causal order and parent set model parameters with the Adam optimiser and learning rate 0.01 for a maximum of 500 iterations and early stopping when improvement stagnates. For the score function estimators, we use a simple exponential moving average with a decay factor of 0.1. Our provided code contains all parameters of our simulation setup in the included `config.py` file.

### B.4 BASELINES

**DDS.** We use the implementation provided by [Charpentier et al. \[2022\]](#) at <https://github.com/sharpenb/Differentiable-DAG-Sampling>. We needed to adapt the hyper-parameters in order to get meaningful results and ran our experiments with the following configuration.

```
# Architecture parameters
'seed_model': 123, # Seed to init model. int
'ma_hidden_dims': [32, 32, 32], # Output dimension. int
'ma_architecture': 'linear', # Output dimension. int
'ma_fast': False, # Output dimension. int
'pd_initial_adj': 'Learned', # Output dimension. int
'pd_temperature': 1.0, # Output dimension. int
'pd_hard': True, # Output dimension. int
'pd_order_type': 'topk', # Output dimension. int
```

```

'pd_noise_factor': 1.0, # Hidden dimensions. list of ints

# Training parameters
'max_epochs': 500, # Maximum number of epochs for training
'patience': 150, # Patience for early stopping. int
'frequency': 2, # Frequency for early stopping test. int
'batch_size': 16, # Batch size. int
'ma_lr': 1e-3, # Learning rate. float
'pd_lr': 1e-2, # Learning rate. float
'loss': 'ELBO', # Loss name. string
'regr': 1e-1, # Regularization factor in Bayesian loss. float
'prior_p': 1e-6 # Regularization factor in Bayesian loss. float

```

**DIBS.** As we build our implementation based on the code provided by [Toth et al. \[2022\]](https://github.com/chritoth/active-bayesian-causal-inference) at <https://github.com/chritoth/active-bayesian-causal-inference>, we use their implementation of DIBS. This also makes results more comparable, as their implementation also uses Gaussian Processes to model mechanisms, which is in contrast to the original implementation by [Lorch et al. \[2021\]](#) based on neural networks. We use their standard parameters with 10 latent particles and constant hyper-parameters  $\alpha = \beta = 1$ .

**BayesDAG.** We use the implementation provided by [Annadani et al. \[2023\]](https://github.com/microsoft/Project-BayesDAG) at <https://github.com/microsoft/Project-BayesDAG>. We needed to adapt the sparsity regularisation hyper-parameter in order to get meaningful results and ran our experiments with the following configuration.

For linear models, we use:

```

"model_hyperparams": {
    "num_chains": 1,
    "sinkhorn_n_iter": 3000,
    "scale_noise_p": 0.001,
    "scale_noise": 0.001,
    "VI_norm": true,
    "input_perm": false,
    "lambda_sparse": 10,
    "sparse_init": false
},
"training_hyperparams": {
    "learning_rate": 1e-3,
    "batch_size": 512,
    "stardardize_data_mean": false,
    "stardardize_data_std": false,
    "max_epochs": 500
}

```

For non-linear Erdős-Rényi models, we use:

```

"model_hyperparams": {
    "num_chains": 1,
    "sinkhorn_n_iter": 3000,
    "scale_noise_p": 0.001,
    "scale_noise": 0.001,
    "VI_norm": true,
    "input_perm": false,
    "lambda_sparse": 10,
    "sparse_init": false
},
"training_hyperparams": {
    "learning_rate": 1e-3,

```



```
"batch_size": 512,
"stardardize_data_mean": false,
"stardardize_data_std": false,
"max_epochs": 500
}
```

For non-linear scale-free models, we use:

```
"model_hyperparams": {
  "num_chains": 1,
  "sinkhorn_n_iter": 3000,
  "scale_noise_p": 0.001,
  "scale_noise": 0.001,
  "VI_norm": true,
  "input_perm": false,
  "lambda_sparse": 10,
  "sparse_init": false
},
"training_hyperparams": {
  "learning_rate": 1e-3,
  "batch_size": 512,
  "stardardize_data_mean": false,
  "stardardize_data_std": false,
  "max_epochs": 500
}
```

As the implementation runs a number of MCMC chains and only evaluates the best chain afterwards, we use only one MCMC chain to enable a fair comparison, as multiple chains would correspond to multiple runs of the other methods.

## C EXTENDED EXPERIMENTAL RESULTS

We provide additional results and ablation studies in Tab. 2.

**Influence of the maximum parent set size.** We evaluate the influence of the maximum parent set size in range  $k \in \{1, 2, 3\}$  in models COM-EX-Kk-GP. As expected,  $k = 1$  performs worst, as each node can only have one parent. Not surprisingly,  $k = 2$  performs best on scale-free graphs, whereas  $k = 3$  performs best on Erdős-Rényi graphs, as the respective  $k$  better fit the structural properties of the true graphs.

**Influence of the expressiveness of the causal order model.** We compare our auto-regressive causal order model, COM-EX-GP, with predicted logits to a simple baseline COM-SIMPLE-EX-GP, where we have  $g_{\theta(Q^L)} = \theta$ , i.e., a constant logit vector  $\theta \in \mathbb{R}^d$ . Surprisingly, the simple baseline performs only slightly worse than our proposed expressive model. In our experiments we observe that, apparently, using 100 causal orders samples for the Monte-Carlo estimates includes at least 1 ‘reasonably good’ order, that is then responsible for the good performance, i.e., the simple models produces a have a winner-takes-all situation because it suffers from weight degeneracy in the importance weights. In contrast, the importance weights for our expressive auto-regressive causal order model are approximately uniform, which indicates that we learn a meaningful proposal distribution.

**Influence of sequential vs. concurrent optimisation.** We compare our model COM-PSM-GP with our sequential optimisation procedure as proposed in § 3.1.4, for that we also report results in the main results in Tab. 1, to models COM-PSM-CONC-GP where the causal order and parent set models are trained simultaneously, i.e., in each optimisation epoch, both models perform one gradient update step. Note, that the concurrent optimisation variant is more truthful to the actual optimisation problem in Eq. (3.4), as the sequential optimisation procedure relies on an approximation to optimise the causal order model. Apparently, the COM-PSM-CONC-GP yields sparser graphs, trading a better TNR for a worse TPR. However, quality of the inferred mechanisms as reflected by the RRMSE is significantly worse than in the sequential optimisation model.

Table 2: Ablation studies on simulated (non-)linear ground truth models with 20 nodes and different DAG structures. We report means and 95% confidence intervals (CIs) across 20 different ground truth models. Best values are bold-faced. As the true graph is not identifiable in the linear scenario, the reported structure learning metrics are computed w.r.t. the skeleton of the true DAG.

| Model            | #Edges | ↓ ESHD | ↑ AUROC     | ↑ AUPRC     | ↑ TPR       | ↑ TNR       | ↑ F1        | ↓ RRMSE     |
|------------------|--------|--------|-------------|-------------|-------------|-------------|-------------|-------------|
| COM-EX-K1-GP     | 15 ± 1 | 27 ± 2 | 0.76 ± 0.03 | 0.62 ± 0.03 | 0.34 ± 0.02 | 0.99 ± 0.00 | 0.49 ± 0.02 | 0.21 ± 0.00 |
| COM-EX-K2-GP     | 26 ± 1 | 22 ± 2 | 0.82 ± 0.03 | 0.73 ± 0.03 | 0.55 ± 0.03 | 0.97 ± 0.01 | 0.66 ± 0.03 | 0.21 ± 0.00 |
| COM-EX-K3-GP     | 34 ± 2 | 21 ± 2 | 0.87 ± 0.02 | 0.77 ± 0.04 | 0.66 ± 0.04 | 0.95 ± 0.01 | 0.71 ± 0.03 | 0.24 ± 0.00 |
| COM-EX-GP        | 26 ± 1 | 22 ± 2 | 0.82 ± 0.03 | 0.73 ± 0.03 | 0.55 ± 0.03 | 0.97 ± 0.01 | 0.66 ± 0.03 | 0.21 ± 0.00 |
| COM-SIMPLE-EX-GP | 25 ± 2 | 23 ± 2 | 0.84 ± 0.02 | 0.73 ± 0.03 | 0.53 ± 0.03 | 0.97 ± 0.01 | 0.64 ± 0.03 | 0.24 ± 0.01 |
| COM-PSM-GP       | 89 ± 6 | 72 ± 4 | 0.66 ± 0.02 | 0.54 ± 0.02 | 0.72 ± 0.04 | 0.60 ± 0.03 | 0.43 ± 0.02 | 1.07 ± 0.06 |
| COM-PSM-CONC-GP  | 52 ± 9 | 48 ± 6 | 0.67 ± 0.02 | 0.53 ± 0.02 | 0.54 ± 0.05 | 0.80 ± 0.05 | 0.47 ± 0.02 | 1.48 ± 0.05 |

(a) Erdős-Rényi Nonlinear.

| Model            | #Edges  | ↓ ESHD | ↑ AUROC     | ↑ AUPRC     | ↑ TPR       | ↑ TNR       | ↑ F1        | ↓ RRMSE     |
|------------------|---------|--------|-------------|-------------|-------------|-------------|-------------|-------------|
| COM-EX-K1-GP     | 18 ± 1  | 22 ± 1 | 0.79 ± 0.02 | 0.69 ± 0.03 | 0.44 ± 0.02 | 0.99 ± 0.00 | 0.59 ± 0.03 | 0.20 ± 0.00 |
| COM-EX-K2-GP     | 32 ± 1  | 13 ± 2 | 0.93 ± 0.02 | 0.87 ± 0.04 | 0.77 ± 0.03 | 0.97 ± 0.01 | 0.81 ± 0.03 | 0.20 ± 0.00 |
| COM-EX-K3-GP     | 40 ± 1  | 19 ± 2 | 0.91 ± 0.02 | 0.84 ± 0.04 | 0.79 ± 0.03 | 0.93 ± 0.01 | 0.75 ± 0.03 | 0.24 ± 0.01 |
| COM-EX-GP        | 32 ± 1  | 13 ± 2 | 0.93 ± 0.02 | 0.87 ± 0.04 | 0.77 ± 0.03 | 0.97 ± 0.01 | 0.81 ± 0.03 | 0.20 ± 0.00 |
| COM-SIMPLE-EX-GP | 31 ± 1  | 14 ± 2 | 0.91 ± 0.02 | 0.85 ± 0.03 | 0.74 ± 0.04 | 0.97 ± 0.01 | 0.79 ± 0.04 | 0.24 ± 0.01 |
| COM-PSM-GP       | 88 ± 4  | 68 ± 4 | 0.69 ± 0.02 | 0.55 ± 0.02 | 0.77 ± 0.03 | 0.61 ± 0.03 | 0.45 ± 0.02 | 1.0 ± 0.04  |
| COM-PSM-CONC-GP  | 68 ± 12 | 55 ± 9 | 0.70 ± 0.02 | 0.56 ± 0.02 | 0.67 ± 0.05 | 0.72 ± 0.07 | 0.48 ± 0.04 | 1.41 ± 0.06 |

(b) Scale-free Nonlinear.

| Model            | #Edges | ↓ ESHD | ↑ AUROC     | ↑ AUPRC     | ↑ TPR       | ↑ TNR       | ↑ F1        | ↓ RRMSE     |
|------------------|--------|--------|-------------|-------------|-------------|-------------|-------------|-------------|
| COM-EX-GP        | 31 ± 2 | 40 ± 4 | 0.68 ± 0.03 | 0.44 ± 0.04 | 0.40 ± 0.03 | 0.90 ± 0.01 | 0.44 ± 0.03 | 0.17 ± 0.00 |
| COM-SIMPLE-EX-GP | 30 ± 2 | 43 ± 4 | 0.66 ± 0.03 | 0.43 ± 0.05 | 0.34 ± 0.03 | 0.89 ± 0.01 | 0.38 ± 0.04 | 0.17 ± 0.00 |
| COM-EX-K3-GP     | 45 ± 2 | 49 ± 4 | 0.65 ± 0.03 | 0.42 ± 0.05 | 0.46 ± 0.04 | 0.82 ± 0.02 | 0.43 ± 0.04 | 0.17 ± 0.00 |

(c) Erdős-Rényi Linear.

| Model            | #Edges | ↓ ESHD | ↑ AUROC     | ↑ AUPRC     | ↑ TPR       | ↑ TNR       | ↑ F1        | ↓ RRMSE     |
|------------------|--------|--------|-------------|-------------|-------------|-------------|-------------|-------------|
| COM-EX-GP        | 34 ± 1 | 47 ± 3 | 0.61 ± 0.03 | 0.33 ± 0.04 | 0.32 ± 0.04 | 0.85 ± 0.01 | 0.33 ± 0.04 | 0.16 ± 0.00 |
| COM-SIMPLE-EX-GP | 34 ± 1 | 48 ± 3 | 0.61 ± 0.03 | 0.31 ± 0.04 | 0.31 ± 0.04 | 0.85 ± 0.01 | 0.31 ± 0.04 | 0.16 ± 0.00 |
| COM-EX-K3-GP     | 48 ± 1 | 57 ± 4 | 0.58 ± 0.04 | 0.29 ± 0.04 | 0.38 ± 0.06 | 0.78 ± 0.01 | 0.32 ± 0.05 | 0.16 ± 0.00 |

(d) Scale-free Linear.